Journal of Magnetic Resonance 214 (2012) 352–359

Contents lists available at SciVerse ScienceDirect

Journal of Magnetic Resonance

journal homepage: www.elsevier.com/locate/jmr

Communication

Fast detection of choline-containing metabolites in liver using 2D ^{1}H–^{14}N three-bond correlation (HN3BC) spectroscopy

Xi-an Mao [a,b,*], Ning Li [c], Jiezhen Mao [a], Qiurong Li [c], Nan Xiao [a], Bin Jiang [a], Ling Jiang [a,*], Xu-xia Wang [a], Maili Liu [a,*]

[a] State Key Laboratory of Magnetic Resonance and Atomic Molecular Physics, Wuhan Institute of Physics and Mathematics, The Chinese Academy of Sciences, Wuhan, Hubei 430071, China
[b] Department of Pharmacology, Case Western Reserve University School of Medicine, Cleveland, OH 44106, USA
[c] Research Institute of General Surgery, Jinling Hospital, Nanjing, Jiangsu 210002, China

ARTICLE INFO

Article history:
Received 10 June 2011
Revised 28 November 2011
Available online 8 December 2011

Keywords:
Choline-containing metabolites
Liver
Carcinoma tissue
Fast detection
^{1}H–^{14}N three-bond correlation spectroscopy

ABSTRACT

Detection and quantification of total choline-containing metabolites (CCMs) in tissues by magnetic resonance spectroscopy (MRS) has received considerable attention as a biomarker of cancer. Tissue CCMs are mainly choline (Cho), phosphocholine (PCho), and glycerophosphocholine (GPCho). Because the methyl ^{1}H resonances of tissue CCMs exhibit small chemical shift differences and overlap significantly in 1D ^{1}H MRS, quantification of individual components is precluded. Development of a MRS method capably of resolving individual components of tissue CCMs would be a significant advance. Herein, a modification of the 2D ^{1}H–^{14}N HSQC technique is targeted on the two methylene ^{1}H in the CH_2O group ($^{3}J_{1H14N}$ = 2.7 Hz) and applied to *ex vivo* mouse and human liver samples at physiological temperature (37 °C). Specifically, the ^{1}H–^{14}N HSQC technique is modified into a 2D ^{1}H–^{14}N three-bond correlation (HN3BC) experiment, which selectively detects the ^{1}H of CH_2O coupled to ^{14}N in CCMs. Separate signals from Cho, PCho, and GPCho components are resolved with high detection sensitivity. A 2D HN3BC spectrum can be recorded from mouse liver in only 1.5 min and from human carcinoma liver tissue in less than 3 min with effective sample volume of 0.2 ml at 14.1 T.

1. Introduction

Human health is threatened by many diseases especially cancer. Recent reports estimated about 570,000 deaths from cancer in the United States in 2010 [1]. When cancer is diagnosed, in many cases it is already in its late stages. Therefore, early cancer detection has become the aim of many projects over the decades. Magnetic resonance spectroscopy (MRS) detection of choline-containing metabolites (CCMs) is one of the most important noninvasive techniques that could provide early detection of cancer and early response to therapy. Investigation of the relationship between CCM levels and cancer using MRS can be traced back to the 1980s [2]. Since then, numerous MRS studies have reported on the possibility that elevation of total choline (*t*Cho) levels could be used for cancer diagnosis [3,4]. However, current *t*Cho detection methods have more or less limitations which sometimes result in low diagnostic sensitivity and specificity [5]. Moreover, conflicting results have been demonstrated between MRS and other imaging methods such as PET [6]. Therefore, some MRS experts [7–10] are only conservatively optimistic about using CCMs as biomarkers for cancer diagnosis. A reliable clinical CCM detection technique should provide spectra or images of high selectivity (not obscured by other signals), high sensitivity (having reasonable signal-to-noise ratio or SNR within patient-acceptable measurement time), high spectral resolution (able to identify individual CCM molecules) and high spatial resolution (with voxel being reasonably small). Unfortunately so far none of the currently available techniques for CCM detection meets all of the criteria.

Recently, we [11,12] introduced the spin-1/2-spin-1 HSQC technique [13–15] to detect CCMs in liquids and tissues. We also pointed out the feasibility of the HSQC technique in clinical applications [12]. The purpose of this work is to improve the HSQC technique and to explore the feasibility of the new technique on *ex vivo* samples at physiological temperature (37 °C). In this study, we modified the ^{1}H–^{14}N HSQC pulse sequence to a ^{1}H–^{14}N three-bond correlation (HN3BC) pulse sequence to enhance the detection sensitivity. This method selectively detects CH_2O protons in CCMs that are coupled to ^{14}N through three chemical bonds, which means that all other protons including the water proton can be cleanly or largely filtered out from the spectrum. As such, this method allows the major compounds in CCMs, *i.e.* choline (Cho),

* Corresponding authors at: Department of Pharmacology, Case Western Reserve University School of Medicine, Cleveland, OH 44106, USA. Fax: +1 216 368 1300.
E-mail addresses: ling.jiang@wipm.ac.cn (L. Jiang), xian.mao@case.edu (X.-a. Mao), ml.liu@wipm.ac.cn (M.L. Liu).

1090-7807/$ - see front matter © 2011 Elsevier Inc. All rights reserved.
doi:10.1016/j.jmr.2011.11.019

phosphocholine (PCho) and glycerophosphocholine (GPCho), to be distinctly measured, and hence can provide information about changes in GPCho/PCho ratio, which is more relevant to cancer diagnosis than *t*Cho [6,16,17]. We believe this method has the potential to become a reliable *in vivo* MRS technique for CCM detection.

2. Materials and methods

Cancerous and normal liver parenchyma tissue samples were obtained from human livers during the surgery for two patients, a 64-year-old male and a 57-year-old female, who were diagnosed by CT with hepatocellular carcinoma. Mouse livers were taken from five healthy C57 Black 6 mice (Jackson Lab., Bar Harbor, Maine). All human and mouse tissue experiments described herein were approved by local Ethical Committees and were strictly following the WMA Declaration of Helsinki. Information consent forms were signed by patients prior to surgery.

All tissue samples were snap-frozen in liquid nitrogen and stored in −80 °C refrigerators. All NMR samples were prepared by transferring the tissues into 5 mm NMR tubes after the samples were thawed. Each NMR tube contained approximately 0.8–1 g of tissue without the addition of any solvent or lock substance. The preparation of an NMR sample took less than 10 min.

For human tissues, each tumor tissue was divided into two NMR samples and we wanted to make sure there was no significant difference in spectra between them. So were the uninvolved normal tissues. Altogether we had five mouse liver samples, four human haptic carcinoma samples and four normal human liver samples.

The HN3BC pulse sequence used in this study is shown in Fig. 1, which is a modification of the conventional $^{1}H–^{14}N$ HSQC pulse sequence [11,12] by inserting two selective refocusing pulses in each INEPT period. Echo–antiecho mode was applied to gradient pulses. A sine bell (a half period of a sine function) was used to shape the gradient pulses with a fixed duration of 1 ms and with the amplitudes of 28 and 2.023 Gauss/cm, whose ratio corresponded to the gamma ratio between ^{1}H and ^{14}N (13.84:1). The shaped pulse "SEDUCE" [18] was used for selective refocusing with 5 ms duration and an offset frequency of 3.58 ppm.

Theoretically the INEPT τ is $1/8J_{HN}$ (with J_{HN} = 2.7 Hz) for 100% polarization transfer from ^{1}H to ^{14}N [11,12,19]. However, in experiments τ was optimized for each sample and each experiment. Typically, τ = 25–30 ms for mouse liver and human liver cancer tissues at 37 °C, τ = 15–20 ms for normal human liver tissues at 37 °C, and τ = 16 ms for mouse liver tissue at 4 °C.

All NMR experiments were performed on Bruker Avance 600 spectrometers (magnetic field = 14.1 T) with ^{14}N resonating at 43.4 MHz. Human samples were measured with a broad band probe at 37 °C. Murine samples were measured with a modified TXI probe at 37 °C or 4 °C with ^{15}N coil replaced by ^{14}N coil (J.S. Research, Boston, MA).

The spectral window for ^{1}H acquisition was either 10 or 6 ppm, while that for ^{14}N was 6 ppm. In the ^{1}H dimension, the frequency carrier was positioned at the water resonance (4.7 ppm) and the chemical shift of the spectrum was calibrated with the CH_2O peak of choline set at 4.07 ppm. In the ^{14}N dimension, the frequency carrier was positioned at the CCM resonances (4.0 ppm), which was calibrated to 48 ppm (indirectly referenced to liquid ammonia). Before the first tissue sample was prepared, the magnetic field was preshimmed carefully with D_2O and the probe was tuned and matched for ^{14}N channel. After the tissue sample was inserted into the magnet, the sample was left alone for 5–10 min to reach a temperature equilibrium, during which the probe was tuned for ^{1}H and the ^{1}H $\pi/2$ pulse was calibrated. No further shimming was performed. Typical experiments for each sample included: 1D ^{1}H NMR with water presaturation (16 scans with TR = 2 s, ~1.5 min), 1D HN3BC NMR with varied INEPT τ for parameter optimization (64 or 128 scans with TR = 1 s, total acquisition time 15–30 min), and 2D HN3BC NMR with optimal τ (TR = 1 s; number of t_1 increment was 16 or 32; 2 scans for mouse liver, 4 or 8 scans for human tumor, 32 or 64 scans for normal human tissue). All experiments for each tissue sample were finished in less than 1 h. The spectra were processed with $\pi/2$-shifted sine square filter in both dimensions. Zero filling was conducted for the indirect dimension to double the number of t_1 increments.

3. Results

The HN3BC pulse sequence showed very high sensitivity in *ex vivo* experiments for the five mouse liver samples at 37 °C. In 1.5 min we were able to obtain a 2D HN3BC spectrum with a SNR around 200 with all three CCMs distinctly separated. All irrelevant signals seen in conventional ^{1}H NMR have been completely removed, along with the water and lipid signals. A typical 2D HN3BC spectrum of mouse liver is shown in Fig. 2B. Compared to 1D ^{1}H NMR (Fig. 2A) which was measured using the same measurement time (1.5 min), the information contained in the 2D HN3BC spectrum is more useful to clinical applications.

To show how much sensitivity was gained in the presence of the selective refocusing pulses, we measured a spectrum (*i.e.* a $^{1}H–^{14}N$ HSQC spectrum) on the same murine sample as in Fig. 2 with the same experimental parameters but without the presence of the selective refocusing pulses. The projection of the $^{1}H–^{14}N$ HSQC spectrum onto the ^{1}H dimension is shown in Fig. 3B and compared with the projection of the HN3BC spectrum shown in Fig. 3A. It is seen that the selective inversion of the NCH_2 magnetizations can enhance the detection by 3.5-fold. To show how much sensitivity was gained by elevating the temperature, we measured two spectra on another murine sample using the HN3BC pulse sequence at different temperatures (37 °C and 4 °C), with their projections displayed in Fig. 4A (37 °C) and 4B (4 °C). It is seen that the sensitivity at higher temperature has been enhanced by a factor of 2.8.

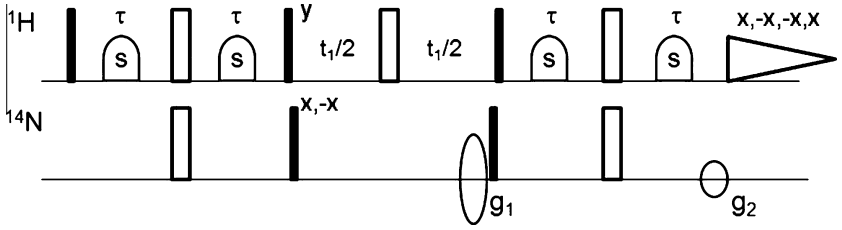

Fig. 1. HN3BC pulse sequence. The filled narrow bars and the open wide bars denote the $\pi/2$ and π pulses, respectively. The arcs labeled "s" denote the shaped π pulses that selectively invert the NCH_2 magnetizations. The ovals denote the gradient pulses that are used for selection of the single quantum coherence of the three-bond ^{1}H-^{14}N coupling pair. Phase cycling is given for two pulses and for data sampling. Other pulses are kept at the same phase as x. Since the ^{1}H-^{14}N coupling constant is very small (2.7 Hz), heteronuclear decoupling is not applied.

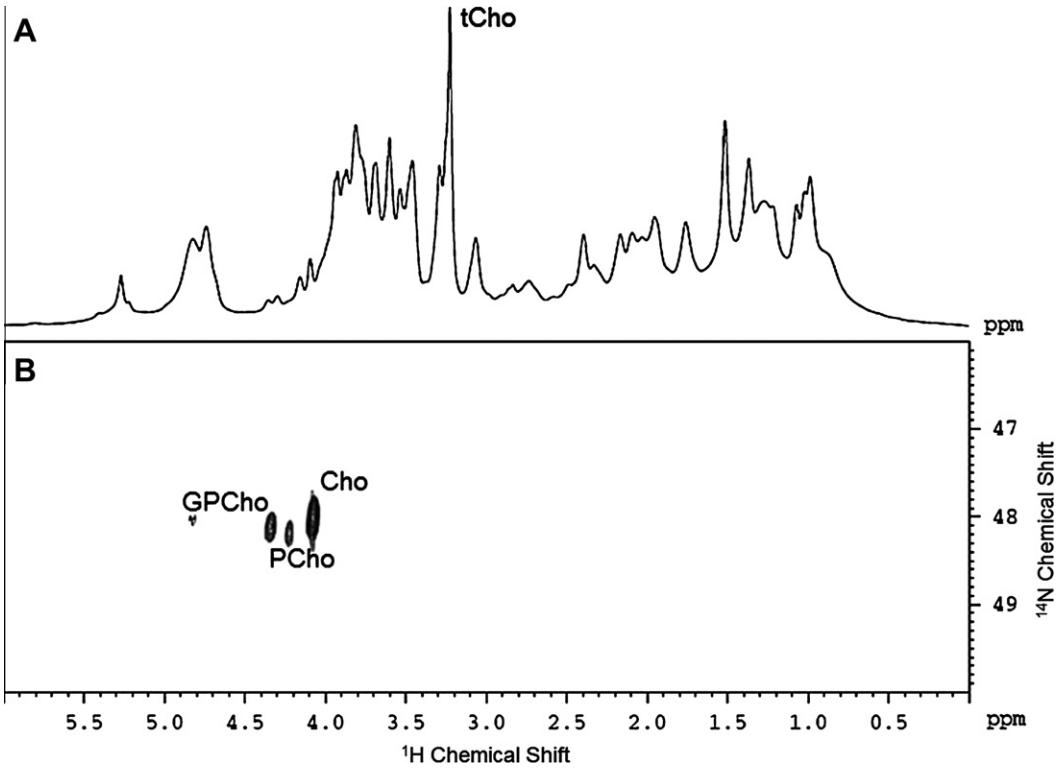

Fig. 2. MR spectra of a mouse liver at 37 °C. (A) Conventional water presaturated ^{1}H MRS. (B) 2D HN3BC MRS (τ_{opt} = 25 ms). Both were measured with the same measurement time (1.5 min). The *t*Cho peak is marked in the 1D spectrum, but it is missing from the 2D HN3BC spectrum because it cannot survive the coherence selection in the HN3BC experiment. In the 2D spectrum there are only three peaks that are unambiguously assigned to the three compounds of CCMs.

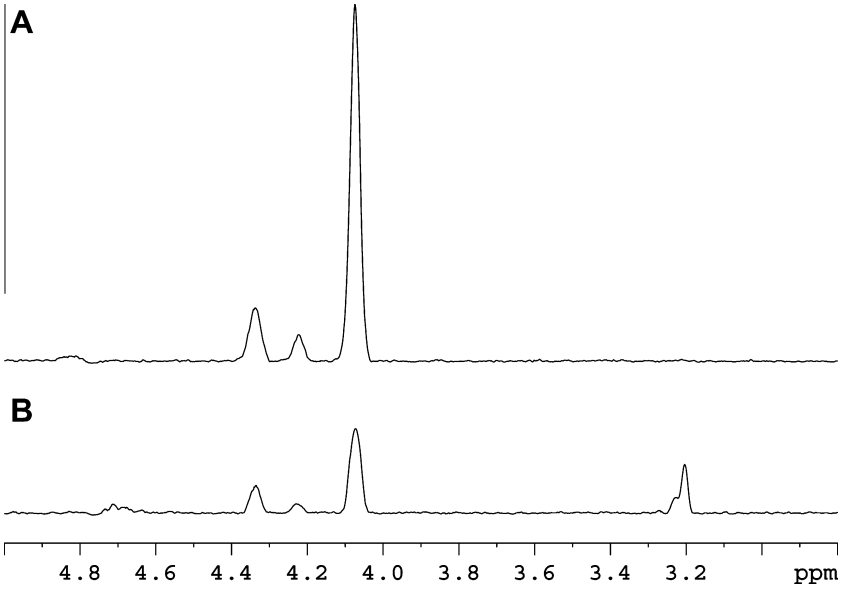

Fig. 3. Projections of two 2D spectra of a mouse liver measured at 37 °C but using different pulse sequences onto the proton dimension. (A) Projection of the HN3BC spectrum (τ = 25 ms) in Fig. 2B. (B) Projection of a ^{1}H-^{14}N HSQC spectrum (τ = 10 ms) measured using the same experimental parameters as in the HN3BC experiment except for the INEPT evolution τ. The intensity ratio between (A) and (B) is about 3.5. Note in particular that the *t*Cho peak at 3.2 ppm in (B) is missing from (A).

The carcinoma spectra of the two patients are presented in Fig. 5A. These spectra are common in that the PCho signal at 4.22 ppm is the dominant peak. As a comparison, the normal tissue spectra of the same patients are presented in Fig. 5B, where the GPCho signal at 4.35 ppm is much higher than the other two CCM signals. The GPCho/PCho ratios measured from the carcinoma spectra in Fig. 5A are respectively, 0.19, 0.26, 0.43 and 0.33, with an average of 0.30. In contrast, the ratios from the normal tissues (Fig. 5B) are respectively 3.5, 4.8, 13.0 and 3.9, with an average of 6.3. These ratios are sufficiently apart to tell whether a test is positive or negative, without involving the complicated problem of choosing water, lipid, creatine or even phantom signals as a quantitative reference. [7].

The conventional 1D ^{1}H MR spectra for the eight human liver samples are presented in Fig. 6, with the carcinoma tissue spectra shown in Fig. 6A and the normal tissue spectra shown in Fig. 6B.

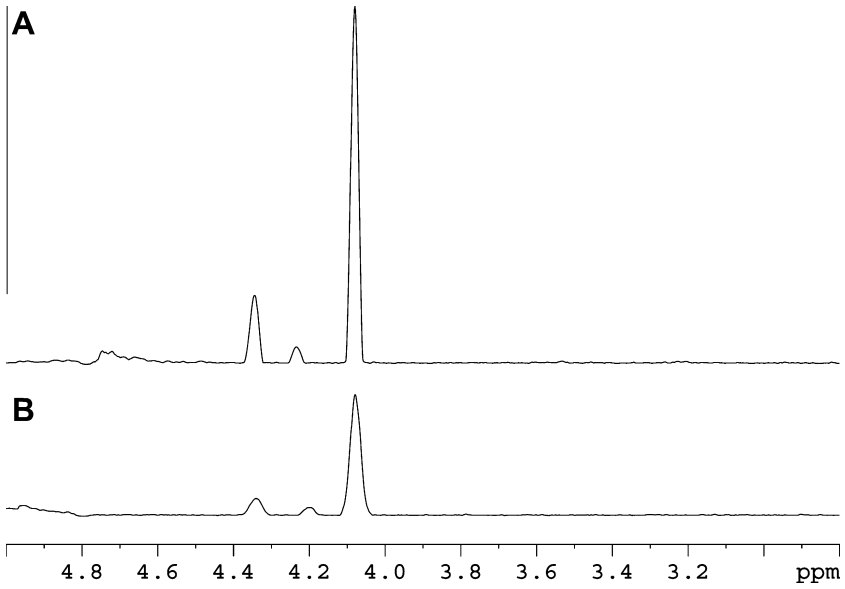

Fig. 4. Projections of two 2D spectra measured using the same pulse sequence (HN3BC) but at different temperatures (37 °C and 4 °C) onto the proton dimension. (A) Spectrum at 37 °C (τ = 25 ms). (B) Spectrum at 4 °C (τ = 16 ms). The integration ratio between (A) and (B) is about 2.8.

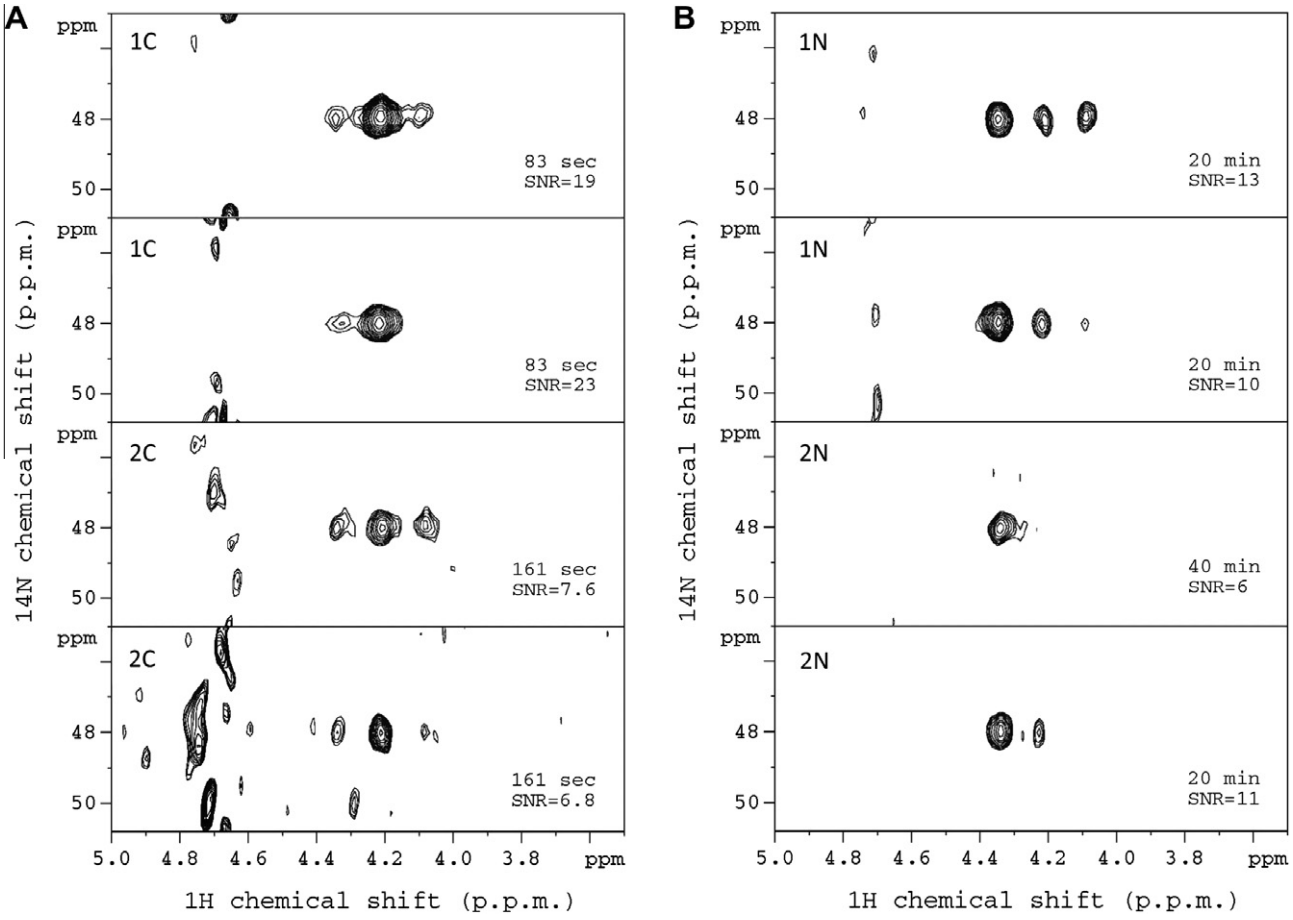

Fig. 5. 2D HN3BC spectra of human liver tissues. (A) From cancer tissues of a 64-year-old male patient (labeled 1c) and a 57-year-old female patient (labeled 2c). (B) From uninvolved tissues adjacent to lesion from the same patients (1n and 2n). Peak assignments are given in the first spectrum of each group. The measurement time and SNR are given in each spectrum, which indicate that the sensitivity of the cancer spectra were much higher than that in normal tissue spectra. In all spectra in (A), the PCho peak is much stronger than the GPCho peak, while in all spectra in (B), the GPCho peak is stronger.

Although the *t*Cho signal in these conventional ^{1}H NMR could also provide information about carcinoma, this information is less straightforward and could be easily obscured by interference from water and lipid resonances.

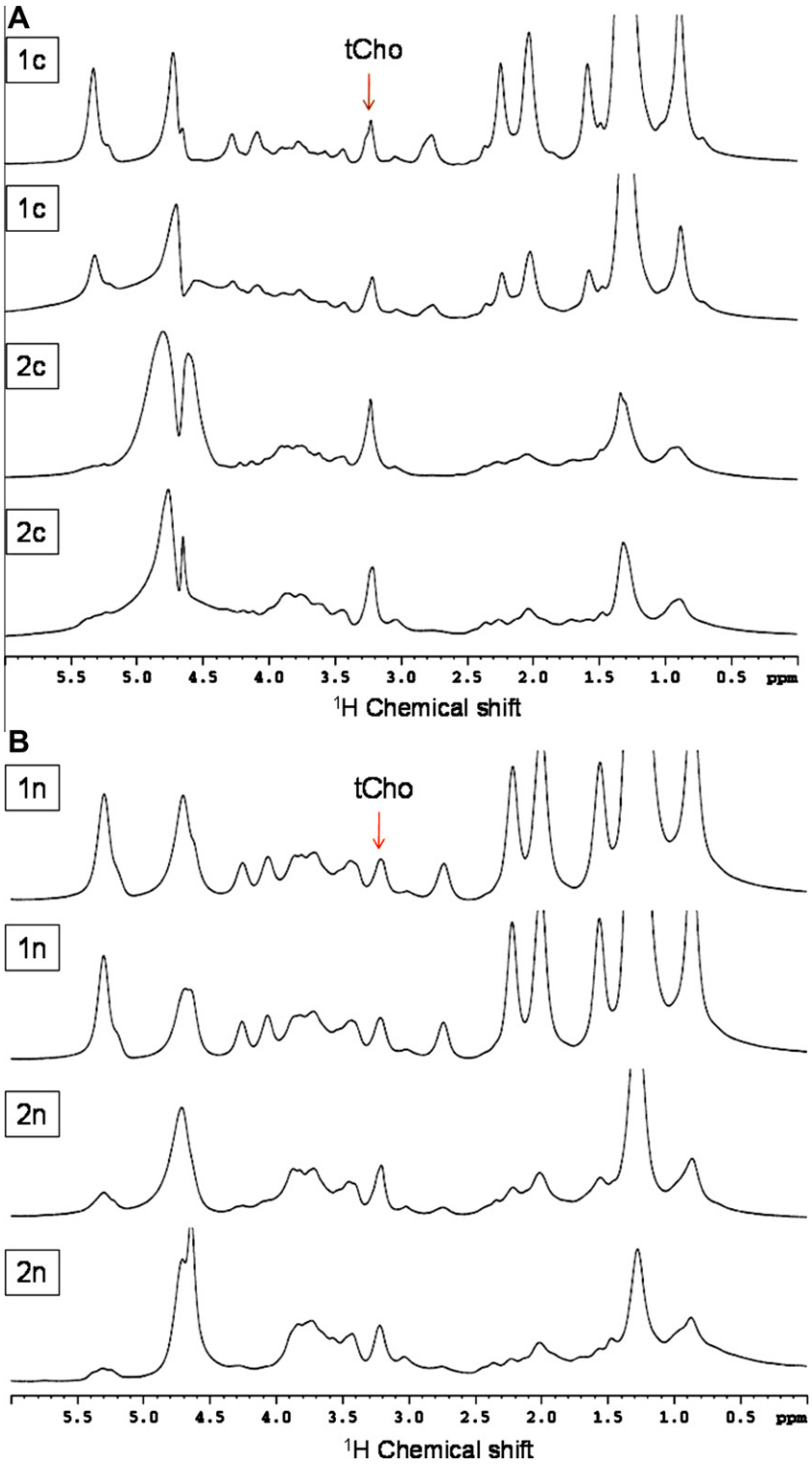

Fig. 6. Water suppressed 1D ^{1}H MR spectra of human liver tissues. (A) From cancer tissues of the same samples as in Fig. 5A. (B) From uninvolved tissues of the same samples as in Fig. 5B. The *t*Cho peak is indicated by an arrow.

4. Discussion

The very high sensitivity of the HN3BC technique results from the combination of a number of factors. In addition to the factors that mentioned in previous studies [11,12], *i.e.*, the rather long (a few seconds) relaxation time of ^{14}N in choline [20], the nearly 100% natural abundance of ^{14}N, and the pulsed field gradients, the selective refocusing pulses employed in the HN3BC pulse sequence play an important role in enhancing the detection sensitivity. With the selective refocusing pulses, the dephasing magnetization due to homonuclear coupling rephrases, thus saving the *J*-losses [21,22]. Furthermore, T_2 losses have been minimized by running experiments at the physiological temperature. In general, T_2 is much longer at higher temperatures than at lower temperatures and longer T_2 is helpful to enhance magnetization transfer. It is the combination of the selective refocusing effect and the temper-

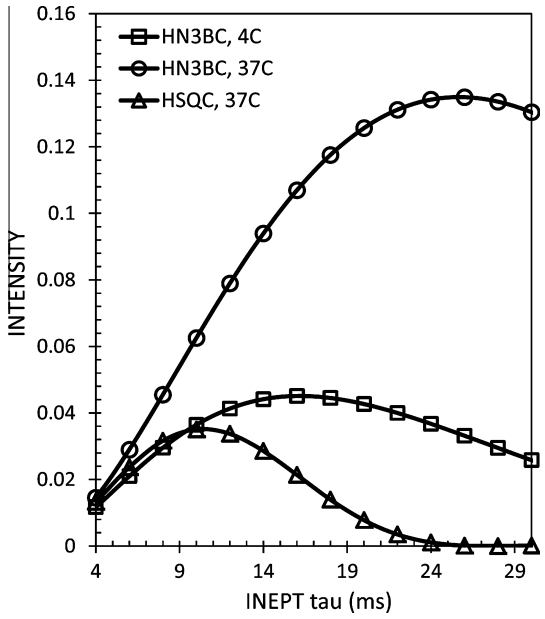

Fig. 7. Simulated intensity curves as a function of the INEPT evolution time (τ) based on Eq. (1). Parameters used for simulation include J_{HN} = 2.7 Hz, $J_{AA'}$ = 9.1 Hz, $J_{AB'}$ = 6.8 Hz, $J_{AB'}$ = 3.3 Hz. For the triangle and circle curves, $T_{2,anti}$ = 70 ms, and for the square curve, $T_{2,anti}$ = 36 ms.

ature-related T_2 effect that can explain why the HN3BC spectrum of mouse liver at 37 °C required only 1.5 min acquisition time.

Semi-quantitatively, the enhancement achieved by improving the pulse sequence and by elevating temperature can be estimated by the simulation demonstrated in Fig. 7 and based on the theory presented below. The $^{1}H–^{14}N$ HSQC signal intensity as a function of coupling constants and the relaxation times can be given by:

$$I = I_0\{\sin(4\pi j_{HN}\tau)[\Pi_{H'}\cos(2\pi j_{HH'}\tau)]\exp(-2\tau/T_{2,H})exp(-2\tau/T_{1,N})\}^2 \quad (1)$$

where I_0 is the intensity when $\tau = 1/8J_{HN}$, $J_{HH'} = 0$, and $T_{2,H} = T_{1,N} = \infty$. The cosine factors in the equation accounts for the homonuclear coupling effect. Since there are two INEPT periods, a square appears in the equation. This equation is similar to the equation proposed for $^{1}H–^{31}P$ HSQC signal intensity [23], but here the contribution from the longitudinal relaxation of ^{14}N is included, since $T_{1,N}$ should be involved in the relaxation of the antiphase coherence $2H_yN_z$. $T_{1,N}$ in the equation well explains why HN3BC or HSQC technique is not feasible for ^{14}N detection of other nitrogen containing molecules: they have very short $T_{1,N}$.

For simplicity, let $1/T_{2,H} + 1/T_{1,N} = 1/T_{2,anti}$, and $T_{2,anti}$ can be measured for the CH_2O protons in CCMs with a new method different from the spin-echo method proposed in Ref. [12]. This new method is through the search for optimal INEPT τ. As homonuclear couplings have been removed by the selective refocusing pulses, the cosine factors in Eq. (1) can be dropped out. Through simple mathematical calculation on Eq. (1), we have

$$T_{2,anti} = (1/2\pi J)\tan(4\pi J\tau_{opt}) \quad (2)$$

Once τ_{opt} is found in experiment, $T_{2,anti}$ can be immediately determined. Eq. (2) can be validated by the data reported in Ref. [12], where τ_{opt} was found to be 12.5 ms, and $T_{2,anti}$ can be evaluated as 26.6 ms using Eq. (2), which was in good agreement with the measured $T_{2,anti}$ (28.5 ms). The optimal τ used for recording the mouse liver HN3BC spectrum at 37 °C (Fig. 2B and Fig. 4A) was 25 ms, which corresponds to $T_{2,anti} \approx 70$ ms. The optimal τ used for recording the mouse liver HN3BC spectrum at 4 °C (Fig. 4B) was 16 ms, which corresponds to $T_{2,anti} \approx 36$ ms.

Simulation with all couplings (coupling constants are taking from Ref. [24]) and with longer relaxation time (70 ms) yields the triangle curve in Fig. 7 (HSQC 37C). The maximum signal intensity is 0.0351, when I_0 is normalized to one. This curve simulates the spectrum presented in Fig. 3B. When homonuclear decoupling is considered and shorter relaxation (36 ms) is assumed, we obtained the square curve (the HN3BC 4C curve), the maximum of which is 0.0451, which simulates the spectrum presented in Fig. 4B. With $T_{2,anti}$ = 70 ms and homonuclear decoupling, we obtained the circle curve (HN3BC 37C) which has a maximum of 0.135, mimicking the high sensitivity in measuring the HN3BC spectrum for mouse liver in Figs. 3B and 4B. Comparison between the maxima of these curves can predict enhancements obtained in experiments. When experiments are performed at 37 °C, homonuclear decoupling can bring about a 3.85-fold enhancement (0.135/0.0351 = 3.85), which has been verified by the spectra in Fig. 3A and B. With homonuclear decoupling (HN3BC), an increase of temperature from 4 °C to 37 °C can lead to a 2.99 (0.135/0.0451 = 2.99) fold enhancement, which has been verified by the 2.8-fold enhancement found in Fig. 4.

It should be pointed out that relaxation times and concentrations of CCMs vary for different mice. $T_{2,anti}$ of a mouse liver at 4 °C measured in Ref. [12] was 28 ms, while $T_{2,anti}$ of a different mouse measured in this work is 36 ms. Comparing the spectrum in Fig. 4B with the spectrum in the previous work [12] suggests that it is very likely that mouse livers used in this study have higher CCM concentrations than the mouse liver measured in Ref. [12].

In the experiments on human liver samples the carcinoma samples showed much higher sensitivity than normal tissue samples, which is understandable, since in cancer tissues the CCM level could be higher [16,17], and T_2 could be longer [25]. Since HN3BC spectra can be obtained from carcinoma samples in less than 3 min while from normal tissue samples in more than 20 min, it is safe to say that we were able to distinguish carcinoma tissues from normal tissues in less than 3 min.

It should be pointed out that the Cho peak in the human liver spectra is very weak compared to the other two peaks, while the Cho peak in the mouse liver spectra is always stronger than the other two. It is very likely that the choline concentration in human liver is relatively low, and perhaps this is the intrinsic nature of human liver. However, it is too early to draw a conclusion. More evidence needs to be collected.

The advantage of the 2D HN3BC technique over the conventional 1D ^{1}H NMR is obvious. First of all, the *t*Cho peak in 1D NMR can be easily obscured by water and lipid signals, as has been demonstrated in many studies, while the water and lipid signals have been largely suppressed in the HN3BC experiments. Secondly, the *t*Cho peak in ^{1}H NMR is contributed not only by the methyl signals of the three compounds in CCMs, but also possibly by phosphosethanolamine and glycerophosphoethanolamine, taurine, trimethylamine-N-oxide, β-glucose and other metabolites, while the three peaks in the HN3NC spectrum are not overlapped by any other signals. Thirdly, it is difficult to choose a reference peak in the ^{1}H MR spectrum for quantification. As can be seen from Fig. 6, it is difficult to find a signal showing constant intensity in all of the eight 1D spectra. Hence *t*Cho is hardly reliable as a diagnostic biomarker. However, in the 2D HN3BC spectrum the three CCM peaks are very well separated and the ratio of GPC/PC can be directly obtained; there is no need to choose a reference peak for quantification.

HN3BC spectroscopy is also comparable to other molecular techniques for CCM detection, such as TOCSY [26], ^{31}P-edited ^{1}H NMR [21], DNP [27–29], and PET [30,31]. TOCSY [26] has pronounced separation ability, as CCMs can also be identified from the well separated CH_2O resonances. However, so far tissue TOCSY experiments have relied on high-resolution magic-angle-spinning

(HR-MAS) [32] for better resolution while HR-MAS is unlikely to become an *in vivo* technique. Furthermore, TOCSY requires high resolution in the indirectly detected dimension with minimally 64 t_1 increments and at least 4 steps of phase cycling, which makes TOCSY a relatively time-consuming experiment. These drawbacks do not exist in HN3BC experiment, as it can be directly applied *in vivo*, requires much fewer t_1 increments (we used only 16 or 32) and requires fewer phase cycling steps (minimally only 2). In addition, the HN3BC spectrum is much cleaner than TOCSY, as far as the CCM detection is concerned.

^{31}P–edited ^{1}H NMR [21] much resembles 1D ^{1}H–^{31}P HSQC and looks to be a promising technique for PC and GPC detection. However, the pulse sequence contains an unnecessary spin-lock pulse that could have seriously attenuated signal intensity. Hence, ^{31}P–edited ^{1}H NMR has not yet developed into a useful clinical technique.

Dynamic nuclear polarization (DNP) technique [27,28] has been proposed for choline detection and is the most sensitive NMR technique. Very recently, DNP was applied to monitoring the enzymatic reactions involved in cancer metabolism and in neuronal transmission [29]. In a typical *in vivo* DNP experiment [28], polarization has to be built up for ^{15}N-labeled choline through the transfer from free radicals at extremely low temperature (1–2 K) for a few hours. Then the polarized ^{15}N-choline has to be injected intravenously. Next, ^{15}N NMR experiment is performed. Although choline-DNP is still under testing, it can be predicted that quantification of the DNP-enhanced choline signal is very difficult, because the signal intensity strongly depends on the efficiency of the polarization transfer from electron spin to nuclear spin, which can vary tremendously between experiments. On the other hand, in DNP experiments described so far, ^{15}N labeled choline has to be used, despite the high sensitivity of hyperpolarization. Positron emission tomography (PET) [30,31] specifically detects choline also without the interference of water and fat, but radio-active choline (^{11}C- or ^{18}F-labeled choline) has to be introduced. Because the lifetimes of these isotopes are short (109 min for ^{18}F and 20 min for ^{11}C), synthesis, purification, injection and patient uptake of the labeled compounds can complicate PET quantification. Compared to DNP and PET, the sensitivity of HN3BC may be lower or even much lower, but the HN3BC method is much simpler and easier to implement. Furthermore, the HN3BC method detects the natural abundant species (*i.e.*, naturally occurred Cho, PCho and GPCho in tissues) which are of physiological significance; it does not need any externally introduced isotope-labeled chemicals.

Just as ^{1}H MRS that has been transferred from *in vitro* to *ex vivo* and to *in vivo*, 2D HN3BC can also be transferred to *in vivo*, at least in principle. Technically, *in vivo* MRS experiments are much more difficult than *ex vivo* high resolution NMR, since the inhomogeneity of both of the B_0 and B_1 fields, plus the movement artifacts, can complicate the measurements. However, the 2D HN3BC technique demonstrated in this paper shows potential in clinical practice, since the sensitivity is very high. In this study, B_0 = 14.1 T, voxel size <0.2 cm^3 (the diameter of the NMR tube was 0.5 cm and the RF coil height was 1 cm; so the effective volume was $3.14 \times 0.25^2 \times 1 = 0.196$ cm^3. If the thickness of the tube wall is assumed to be 0.02 cm, the effective volume was only 0.166 cm^3), and SNR was between 7 and 20. It can be estimated that, on a 3T MRI scanner, a 2D HN3BC spectrum from a voxel of 8 cm^3 can be obtained in less than 10 min, once ^{14}N surface coils are available.

5. Conclusion

^{1}H–^{14}N three-bond correlation (HN3BC) spectroscopy has been proposed and preliminary tested on animal and human liver tissues. A HN3BC spectrum has been obtained from human carcinoma tissues in less than 3 min at 14.1 T with voxel of 0.2 ml and with SNR > 5. In the HN3BC spectrum the three peaks of Cho, PCho and GPCho are well separated, which are suitable for clinical application. This technique has already manifested itself as a useful *ex vivo* clinical tool. However, it can be readily combined with HR-MAS to enhance the sensitivity and resolution of *ex vivo* detection, and with MRI to become a new and useful *in vivo* clinical tool. When *in vivo* HN3BC is successful, HN3BC-MRSI will be the next step, potentially showing sharper contrast between tumor and adjacent uninvolved tissues than conventional MRI, because the sharpness is brought about not only by CCM level difference but also by T_2 difference. As longer T_2 can result in stronger HN3BC signals, commonly used contrast agents for MRI may not be needed.

Acknowledgments

The authors thank National Natural Science Foundation of China (Grants #20635040, #90813017, #20921004, and #21005085) and National Major Basic Research Program of China (Grant #2009CB918603) for financial support. The authors are also grateful to Dr. Michael Zagorski (Professor in the Chemistry Department of CWRU) and Dr. Chris Flask (Professor in University Hospital of CWRU) for their critical reading and English editing.

References

[1] National Cancer Society, Cancer Facts and Figures, 2010, Page 2, <http://www.cancer.org/Research/CancerFactsFigures/index>.
[2] P.F. Daly, J.S. Cohen, Magnetic resonance spectroscopy of tumors and potential in vivo clinical applications: a review, Cancer Res. 49 (1989) 770–779. and references therein.
[3] K. Glunde, M.A. Jacobs, Z.M. Bhujwalla, Choline metabolism in cancer: implications for diagnosis, Expert Rev. Mol. Diagn. 6 (2006) 821–829.
[4] M. Van der Graaf, In vivo magnetic resonance spectroscopy: basic methodology and clinical applications, Eur. Biophys. J. 39 (2010) 527–540.
[5] Y.T. Kuo, C.W. Li, C.Y. Chen, J. Jao, D.K. Wu, G.C. Liu, In vivo proton magnetic resonance spectroscopy of large focal hepatic lesions and metabolite change of hepatocellular carcinoma before and after tanscathelter arterial chemoembolization using 3.0 T MRI scanner, J. Magn. Reson. Image 19 (2004) 598–604.
[6] S. Kwee, T. Ernst, Total choline at ^{1}H-MRS and [^{18}F] Fluromethylcholine uptake at PET, Mol. Image Biol. 12 (2010) 424–425.
[7] F. Podo, F. Sardanelli, E. Iorio, R. Canese, G. Carpinelli, A. Fausto, S. Canevari, Abnormal choline phospholipid metabolism in breast and ovary cancer: molecular bases for noninvasive imaging approaches, Curr. Med. Image Rev. 3 (2007) 123–137.
[8] F. Fischbach, H. Bruhn, Assessment of in vivo ^{1}H magnetic resonance spectroscopy in the liver: a review, Liver Intern. 28 (2008) 297–307.
[9] A.D. Waldman, A. Jackson, S.J. Price, C.A. Clark, T.C. Booth, D.P. Auer, P.S. Tofts, D.J. Collins, M.O. Leach, J.H. Reeset, Quantitative imaging biomarkers in neuro-oncology, Nat. Rev. Clin. Oncol. 6 (2010) 445–454.
[10] S. Kyriazi, S.B. Kaye, N.M. DeSouza, Imaging ovarian cancer and peritoneal metastases-current and emerging techniques, Nat. Rev. Clin. Oncol. 7 (2010) 381–393.
[11] J.Z. Mao, L. Jiang, B. Jiang, M.L. Liu, X.A. Mao, ^{1}H–^{1}4N HSQC detection of choline-containing compounds in solutions, J. Magn. Reson. 206 (2010) 157–160.
[12] J.Z. Mao, L. Jiang, B. Jiang, M.L. Liu, X.A. Mao, A selective NMR method for detecting choline containing compounds in liver tissue: the ^{1}H–^{1}4N HSQC experiment, J. Am. Chem. Soc. 132 (2010) 17349–17351.
[13] Z. Gan, Measuring amide nitrogen quadrupolar coupling by high-resolution N-14/C-13 NMR correlation under magic-angle spinning, J. Am. Chem. Soc. 128 (2006) 6040–6041.
[14] S. Cavadini, A. Lupulescu, S. Antonijevic, G. Bodenhausen, Nitrogen-14 NMR spectroscopy using residual dipolar splittings in solids, J. Amer. Chem. Soc. 128 (2006) 7706–7707.
[15] S.C. Shekar, J.M. Backer, M.E. Girvin, Effectively doubling the magnetic field in spin-1/2-spin-1, HSQC, HDQC, coupled HSQC, and coupled HDQC in solution NMR, J. Chem. Phys. 128 (2008). 184501-1.
[16] E.O. Aboagye, Z.M. Bhujwalla, Malignant transformation alters membrane choline phospholipid metabolism of human mammary epithelial cells, Cancer Res. 59 (1999) 80–84.
[17] E. Ackerstaff, K. Glunde, Z.M. Bhujawlla, Choline phospholipid metabolism: a target in cancer cells?, J Cell. Biochem. 3 (2003) 525–533.
[18] M.A. McCoy, L. Mueller, Selective shaped pulse decoupling in NMR – homonuclear [^{13}C] carbonyl decoupling, J. Am. Chem. Soc. 114 (1992) 2108–2112.

[19] O. Millet, D.R. Muhiram, N.R. Skrynnikov, L.E. Kay, Deuterium spin probes of side-chain dynamics in proteins. 1. Measurement of five relaxation rates per deuteron in ^{13}C-labeled and fractionally ^{2}H-enriched proteins in solution, J. Am. Chem. Soc. 124 (2002) 6439–6448.
[20] M.P. Gamcsik, I. Constantinidis, J.D. Glickson, In vivo ^{14}N nuclear magnetic resonance spectroscopy of tumours-detection of ammonium and trimethylamine metabolites in the murine radiation-induced fibrosarcoma-1, Cancer Res. 51 (1991) 3378–3383.
[21] N.M. Leoning, A.M. Chamberlin, A.G. Zepeda, R.G. Gonzalez, L.L. Cheng, Quantification of phosphocholine and glycerophosphocholine with ^{31}P edited ^{1}H NMR spectroscopy, NMR Biomed. 18 (2005) 413–420.
[22] A. Mohebbi, O. Gonen, Recovery of heteronuclear coherence-transfer efficiency losses due to ^{1}H–^{1}H J coupling in proton to phosphorus RINEPT, J. Magn. Reson. Ser. A 123 (1996) 237–241.
[23] L. Mancini, G.S. Payne, M.O. Leach, Comparison of polarization transfer sequences for enhancement of signals in clinical ^{31}P MRS studies, Magn. Reson. Med. 50 (2003) 578–588.
[24] V. Govindaraju, K. Young, A.A. Maudsley, Proton NMR chemical shifts and coupling constants for brain metabolites, NMR Biomed. 13 (2000) 129–153.
[25] R. Damadian, Tumor detection by nuclear magnetic resonance, Science 171 (1971) 1151–1153.
[26] M.G. Swanson, K.R. Keshari, Z.L. Tabatabai, J.P. Simko, K. Shinohara, P.R. Carroll, A.S. Zektzer, J. Kurhanewicz, Quantification of choline- and ethanolamine-containing metabolites in human prostate tissues using ^{1}H HR-MAS total correlation spectroscopy, Magn. Reson. Med. 60 (2008) 33–40.
[27] C. Gabellieri, S. Reynolds, A. Lavie, G.S. Payne, M.O. Leach, T.R. Eykyn, Therapeutic target metabolism observed using hyperpolarized ^{15}N choline, J. Am. Chem. Soc. 130 (2008) 4598–4599.
[28] C. Cudalbu, A. Comment, F. Kurdzesau, R.B. Van Heeswijk, R. Gruetter, Feasibility of in vivo ^{15}N MRS detection of hyperpolarized ^{15}N labeled choline in rats, Phys. Chem. Chem. Phys. 12 (2010) 5818–5823.
[29] T. Harris, P. Giraudeau, L. Frydman, Kinetics from indirectly detected hyperpolarized NMR spectroscopy by using spatially selective coherence transfers, Chem. Eur. J. 17 (2011) 697–703.
[30] H. Watanabe, M. Kanematsu, H. Kondo, N. Kako, N. Yamamoto, T. Yamada, S. Goshima, H. Hoshi, K.T. Bae, Preoperative detection of prostate cancer: a comparison with ^{11}C-choline PET, ^{18}F-fluorodeoxyglucose PET and MR imaging, J. Magn. Reson. Image 31 (2010) 1151–1156.
[31] K. Mertens, D. Slaets, B. Lambert, M. Acou, F. De Vos, I. Goethals, PET with ^{18}F-labelled choline-based tracers for tumor imaging: a review of the literature, Eur. J. Nucl. Med. Mol. Image 37 (2010) 2188–2193.
[32] B. Sitter, F. Ton, T.F. Bathen, M.B. Tessem, I.S. Gribbestad, High resolution magic angle spinning (HR-MAS) MR spectroscopy in metabolic characterization of human cancer, Prog. NMR Spectrosc. 54 (2009) 239–254.